Functional Consequences of Wnt-Induced Dishevelled2 Phosphorylation in Canonical and Non-Canonical Signaling*

José M. González-Sancho[1§†], Yoshimi Endo Greer[2§], Cristina L. Abrahams[1], Yutaka Takigawa[1], Bolormaa Baljinnyam[2], Kyung Ho Lee[3], Kyung S. Lee[3], Jeffrey S. Rubin[2] and Anthony M.C. Brown[1¶]

[1]Department of Cell and Developmental Biology, Weill Cornell Medical College, New York, NY 10065, USA

[2] Laboratory of Cellular and Molecular Biology and [3]Laboratory of Metabolism, Center for Cancer Research, National Cancer Institute, National Institutes of Health, Bethesda, MD 20892, USA

*Running title: *Wnt-induced phosphorylation sites in Dvl2 regulate signaling*

[¶]To whom correspondence should be addressed: Anthony M.C. Brown, Department of Cell and Developmental Biology, Weill Cornell Medical College, 1300 York Avenue, New York, NY 10065, USA, Tel.: (646) 962-2214; Fax: (212) 879-2733; E-mail : amcbrown@med.cornell.edu

[†]Present Address: Instituto de Investigaciones Biomédicas "Alberto Sols", Consejo Superior de Investigaciones Científicas-Universidad Autónoma de Madrid, Madrid, E-28029, Spain.

[§]These authors contributed equally to this work.

Keywords: Wnt; Dishevelled; phosphorylation; CK1δ; CK1ε; canonical, non-canonical

---

Background: Wnt signaling causes phosphorylation of Dishevelled, but its functional significance is unclear.
Result: Sites of Wnt-induced phosphorylation were mapped in Dvl2 and mutated to permit functional testing.
Conclusion: Three CK1 phosphorylation sites in the C-terminal of Dvl2 account for the Wnt induced mobility shift and modulate signaling.
Significance: Wnt-induced phosphorylation of Dvl differentially regulates canonical and non-canonical Wnt signaling.

SUMMARY

Dishevelled (Dvl) proteins are intracellular effectors of Wnt signaling that have essential roles in both canonical and non-canonical Wnt pathways. It has long been known that Wnts stimulate Dvl phosphorylation, but relatively little is known about its functional significance. We have previously reported that both Wnt3a and Wnt5a induce Dvl2 phosphorylation that is associated with an electrophoretic mobility shift and loss of recognition by monoclonal antibody 10B5. In the present study, we mapped the epitope to a 16-amino acid segment of human Dvl2 (residues 594-609) that contains four Ser/Thr residues. Alanine substitution of these residues (P4m) eliminated the mobility shift induced by either Wnt3a or Wnt5a. The Dvl2 P4m mutant showed a modest increase in canonical Wnt/β-catenin signaling activity relative to wild-type. Consistent with this finding, Dvl2 4Pm preferentially localized to cytoplasmic puncta. In contrast to wild-type Dvl2, however, the 4Pm mutant was unable to rescue Wnt3a-dependent neurite outgrowth in TC-32 cells following suppression of endogenous Dvl2/3. Earlier work has implicated casein kinase 1δ/ε as responsible for the Dvl mobility shift, and a CK1δ in vitro kinase assay confirmed that Ser594, Thr595 and Ser597 of Dvl2 are CK1 targets. Alanine substitution of these 3 residues was sufficient to

abrogate the Wnt-dependent mobility shift. Thus, we have identified a cluster of Ser/Thr residues in the C-terminal domain of Dvl2 that are Wnt-induced phosphorylation (WIP) sites. Our results indicate that phosphorylation at the WIP sites reduces Dvl accumulation in puncta, and attenuates β-catenin signaling, while it enables non-canonical signaling that is required for neurite outgrowth.

Dishevelleds (Dvls) are multifunctional intracellular proteins that were first identified through their essential role in the transduction of signals elicited by members of the Wnt family of secreted proteins (1-3). Wnt proteins themselves are widely known critical regulators of embryonic and postnatal development. They control diverse aspects of cell behavior including cell polarity and stem cell self-renewal, and aberrant Wnt signaling is associated with numerous human diseases, including cancer (4,5).

Intracellular signaling triggered by Wnt proteins is generally classified in two functional categories: canonical and non-canonical, based on the involvement of β-catenin as a signaling intermediate (5,6). Canonical Wnt signaling is initiated by binding of Wnt proteins to a Frizzled-LRP5/6 receptor complex (7). This leads to stabilization of cytoplasmic β-catenin by inhibiting phosphorylation events that otherwise target the protein for proteasomal destruction. The stabilized β-catenin also accumulates in the nucleus where, together with Tcf/Lef proteins, it regulates the transcription of specific target genes (5,7). Wnt1 and Wnt3a are examples of Wnt ligands that typically activate canonical Wnt/β-catenin signaling (8), although they also stimulate other Wnt signaling pathways (9-12).

In contrast to the above mechanism, non-canonical Wnt signaling can be broadly defined as an intracellular response to Wnt proteins that does not involve stabilization of β-catenin. There are numerous instances of such signaling in development, particularly associated with planar cell polarity (PCP) and the movement of cells during morphogenesis (6,13). More recent data also implicate non-canonical Wnt signaling in the regulation of tumor cell invasiveness and motility (14-17). Wnt5a is currently the best-studied Wnt protein that usually signals via non-canonical mechanisms (17,18). Through genetic and biochemical studies in diverse organisms, several pathways of non-canonical Wnt signaling have been proposed, such as the Wnt/PCP, Wnt/Ca2+, and Wnt/Ror2 pathways (19-22). However, many details of these pathways remain obscure and there may be additional non-canonical signaling mechanisms.

Dishevelled (Dvl) proteins are among the few signaling intermediaries common to both modes of Wnt signaling, canonical and non-canonical. In mammals there are three isoforms, Dvl-1, 2, and 3, which are products of paralogous genes. Each has a conserved domain structure comprising DIX, PDZ, and DEP domains, followed by a C-terminal domain (CTD) (3). Several other proteins can bind Dvls and the latter have thus been referred to as scaffold proteins (3,23). Dvl proteins also have a capacity to form multimeric complexes and this can be promoted by Wnt signaling (24-26). In canonical signaling, such multimers may be recruited to Wnt receptors to form signalosomes, which, in turn, recruit Axin and other proteins that inactivate the β-catenin destruction complex (27,28).

All three mammalian Dvl proteins become phosphorylated in response to Wnt signals, a feature that is detectable as a mobility shift on SDS-polyacrylamide gels (12,29). Although the phosphorylated and shifted form ('psDvl') has sometimes been assumed to be a sign of 'activation' in terms of downstream signaling, the kinetics of Wnt-induced Dvl phosphorylation appear too slow to be able to precede the stabilization of β-catenin in canonical signaling (12,30-33). Moreover, we and others have shown that Dvl becomes phosphorylated, not only in response to Wnts that stimulate the canonical pathway, but also in response to those such as Wnt5a that do not stabilize β-catenin (12,30,33,34). As Wnt-induced phosphorylation of Dvl can occur in the absence of β-catenin stabilization, and is independent of the LRP5/6 Wnt receptor components required for canonical Wnt signaling, we have previously argued that psDvl is a manifestation of non-canonical Wnt signaling (12). However, the functional consequences of Dvl phosphorylation for either mode of Wnt signal transduction have remained unclear.

Several kinases have been reported to bind and/or phosphorylate Dvl, including casein kinase

1 delta and epsilon (CK1δ/ε), casein kinase 2, PAR-1, Plk1, and protein kinase C (reviewed in (3)). Dozens of phosphorylation sites have been documented in Dvl proteins, and some have been identified as targets of specific kinases (35-38). While phosphorylation sites are widely distributed in the Dvl sequence, they are particularly abundant in the CTD (35). Deletion analysis and site-directed mutagenesis have suggested that phosphorylation in this region correlates with formation of psDvl (12,35,39). Furthermore, it has been proposed that CK1δ/ε are primarily responsible for CTD phosphorylation and the corresponding mobility shift (39). However, CK1 is able to phosphorylate other Wnt signaling components besides Dvl, and regulates their function (40,41). Thus it has proved difficult to investigate functional consequences of Dvl phosphorylation in isolation from pleiotropic effects of altered kinase levels.

In the present study we identify a cluster of three Ser/Thr residues in Dvl2 that constitutes a key target of Wnt-induced phosphorylation in vivo and is a target for CK1 phosphorylation in vitro. Mutation of the three amino acids to Ala prevents the shift in electrophoretic mobility of Dvl2 in response to either Wnt3a or Wnt5a. Our data further indicate that the Wnt-induced phosphorylation normally observed at these residues in wild-type Dvl results in attenuation of canonical Wnt signaling and concomitant stimulation of non-canonical activity.

EXPERIMENTAL PROCEDURES

Cell culture and neurite outgrowth. Rat2 fibroblasts and HEK293T cells were maintained in Dulbecco's modified Eagle medium containing 10% fetal bovine serum (FBS; Life Technologies). C57MG cells were cultured in the same medium supplemented with 10 μg/ml insulin (Invitrogen). The ESFT cell line TC-32 was grown on cell culture dishes, cluster plates or glass coverslips pre-coated with type I collagen solution (Sigma-Aldrich, St. Louis, MO) as described (10). Wnt-stimulated neurite outgrowth was induced and quantified as previously described (10).

Recombinant protein and conditioned medium. Recombinant Wnt3a was purchased from R&D Systems (Minneapolis, MN). Secreted Frizzled-Related protein (sFRP-1) was prepared as described (42). Wnt5a CM was harvested from Rat2/Wnt5a cells in DMEM + 1% FBS, centrifuged at 2000 x g for 10 min, and concentrated 10-fold using Centriplus YM-10 columns (Millipore). Wnt3a CM was obtained from L/Wnt3a cells as previously described (12).

Antibodies used for Western blotting. Mouse anti-Dvl-2 (10B5), rabbit anti-Dvl-2 (H-75), mouse anti-Myc (9E10), and mouse anti-HSP70 were from Santa Cruz Biotechnology (Santa Cruz, CA). Rabbit anti-Dvl2 (cat#3216) and rabbit anti-Dvl3 (cat#3218) were from Cell Signaling Technology, Inc (Danvers, MA). Mouse anti-β-catenin (C19220) and mouse anti-GSK3β (clone 7) were from BD Transduction Labs (San José, CA). Mouse FLAG (M2) antibody was obtained from Sigma-Aldrich.

Immunoblotting. For Western blot analysis of Rat2 and HEK293T cells, lysates were prepared in RIPA buffer and processed as previously described (12). Separation of phosphorylated forms of Dvl was achieved using 7% polyacrylamide gels in Tris-glycine buffer. For verification of siRNA-knockdown of endogenous proteins, TC-32 cells transfected with siRNA were harvested 48 h after transfection and processed for SDS-PAGE and Western blot analysis as previously described (10).

Recombinant DNA. Human Dvl2 cDNA was cloned into pcDNA3.1-mycHisA (Invitrogen) using NotI and XhoI sites. hDvl2 deletion constructs were then generated by PCR using 3'-specific primers. Site-directed mutagenesis for production of hDvl mutants was performed using a QuikChange II Mutagenesis Kit (Agilent Technologies, Inc. Santa Clara, CA) and all mutations were verified by DNA sequencing. Myc-tagged hDvl2 mutants and WT were sub-cloned into the retroviral vector pLNCX, using SnaBI and StuI sites, for stable expression in Rat2 cells (see below). pCS2+ FLAG-mDvl2 WT was kindly provided by X. He (Harvard University) and mDvl2 P4m was generated from this by site-directed mutagenesis as above. pcDNA3.3 Myc-tagged mCK1δ and mCK1ε were prepared as described (43). For pCMV32 lentiviral constructs Gateway entry clones were first generated from pCS2+ FLAG-mDvl2 WT and P4m and lentiviral expression clones were then constructed using Multisite Gateway recombinational cloning (Invitrogen).

Retroviral and lentiviral expression. LNCX retroviral vectors expressing Myc-tagged WT or mutant hDvl2 were packaged in BOSC23 cells, and the viruses used to transduce Rat2 cells with selection in G418 (Geneticin) (44). Lentiviral particles were produced by transient transfection of HEK293T cells and concentrated 10-fold with Amicon Ultra-15 (Millipore, Billerica, MA). For lentiviral transduction, TC-32 cells at 80-90% confluency in a 6 well plate were infected with 0.2 ml of concentrated lentivirus in 1 ml of medium and 8 μg/ml polybrene (Millipore) and left for 24 h. Selection was performed in Geneticin (400 μg/ml) and the cells subjected to Western blotting to verify recombinant protein expression.

DNA transfection and TOPflash assays. For 10B5 epitope mapping, HEK293T cells were transiently transfected with Myc-tagged hDvl2 deletion constructs in pcDNA3.1 using the DNA-calcium phosphate co-precipitation method and harvested 48 h later for immunoblotting as described above. TOPflash assays were performed by transfection of 293T cells with FuGENE (Promega) using a Dual Luciferase Reagent kit (Promega) largely as described previously (45,46). Plasmid pMT23-β-catenin (46) was used as a positive control for canonical Wnt signaling. Tcf-mediated reporter activity was normalized to the activity of pRL-TK.

DNA transfection and analysis of endogenous gene expression by quantitative PCR. C57MG cells were transfected with pCS2 (empty vector), pCS2+ FLAG-mDvl2 WT or P4m using the Neon Transfection System (Invitrogen). 10^6 cells were placed in 100 μl resuspension buffer and combined with 1 μg of plasmid. Electroporation was performed with two pulses having a width range of 20 ms and 1400 V. Transfected cells were resuspended in 500 μl growth medium and divided into two wells of a 6-well plate, each containing 2 ml growth medium. After 24 h, medium was replaced with DMEM lacking supplements and 1 h later cells were treated for 6 h with 50 ng/ml Wnt3a or bovine serum albumin (BSA, 8 μg/ml) as carrier protein control. RNA was isolated with RNeasy Kit (Qiagen) and cDNA generated with QuantiTect Reverse Transcription Kit (Qiagen). Quantitative PCR was performed as previously described (47). β-actin was quantified in each cDNA sample to normalize results. Data analysis was performed with MxPro software.

siRNA transfection. Dvl2 siRNA targeting the 3'UTR sequence of human Dvl2 was from Qiagen (Valencia, CA); Dvl3 pooled siRNA and Luc siRNA was from Dharmacon (Lafayette, CO). siRNA transfection of TC-32 cells was performed with the Amaxa system (Amaxa, Cologne, Germany) according to the manufacturer's protocol, using 200 pmol of siRNA/10^6 cells. Effects of siRNA treatment were analyzed 48 h after transfection.

Immunofluorescence analysis and antibodies. TC-32 cells were seeded on collagen-coated glass coverslips (Fisher, Pittsburgh, PA) in complete growth medium. Fixation and staining were performed as previously described (10). Mouse FLAG (M2) antibody was from Sigma-Aldrich and Alexa Fluor 488 goat anti-mouse IgG was from Invitrogen. Fluorescent images were collected as described (43)

In vitro kinase assay and mass spectrometry analysis. Mouse Dvl2 cDNA was generated by PCR from pCS2+-Flag-mouse Dvl2 (a gift of S. B. Lee, National Institutes of Health, Bethesda, MD) and cloned into a pGEX-4T-2 vector (Amersham Biosciences, Piscataway, NJ). Similarly, a *Sma*I-*Not*I fragment of human CK1δ was generated by PCR from pCS2+-Myc6-CK1δ (a gift of D. Virshup, Duke-NUS Graduate Medical School, Singapore) and inserted into pGEX-4T-2. GST-Dvl2 and GST-CK1δ were purified from *E. coli* BL21 (DE3) with glutathione (GSH)-agarose (Sigma). *In vitro* kinase reactions were carried out in 50 mM Tris-Cl (pH 7.5), 10 mM $MgCl_2$, 5 mM dithiothreitol, 2 mM EGTA, 0.5 mM Na_3VO_4, and 20 mM *p*-nitrophenyl phosphate in the presence of 100 μM ATP at 30°C for 30 min. Samples were separated by 10% SDS-PAGE. The GST-Dvl2 band was excised and in-gel digested with trypsin (Promega). Tryptic peptides were separated using nanoflow reversed-phase liquid chromatography, coupled online to an LTQ linear ion trap or LTQ-Orbitrap XL mass spectrometer (Thermo Electron, San Jose, CA) for MS/MS and MS/MS/MS analysis. The mass spectrometer was operated in a data-dependent mode to sequentially acquire MS, MS^2 and neutral phosphate loss-dependent MS^3 spectra with dynamic exclusion. Normalized collision energy was 35% for both MS^2 and MS^3.

The raw MS^2 and MS^3 data were searched using SEQUEST (Thermo Electron) to identify phosphopeptides. These were subjected to validation of peptide sequence and phosphorylation sites by examining the corresponding MS^2 and/or MS^3 spectra.

Statistical analysis. The significance of differences in data was determined with Student's t-test. Differences were considered significant when p value was less than 0.05.

RESULTS

Mapping Wnt-induced phosphorylation sites in Dvl2 associated with mobility shift. The phosphorylation of Dvl induced by Wnt signaling results in altered mobility of the protein with the phosphorylated-and-shifted form, psDvl, being noticeably retarded on polyacrylamide gels. We have previously reported that the Dvl2 monoclonal antibody (mAb) 10B5 is selectively deficient in recognizing psDvl2, although it readily detects the unmodified, or faster migrating, band (12). This phenomenon is illustrated in Figure 1A, both for endogenous Dvl2 in Rat2 cells and for exogenous Myc-tagged human Dvl2. The inability of 10B5 to detect psDvl2 suggests that the epitope is masked by Wnt-induced phosphorylation. To identify the site of this phosphorylation, we mapped the 10B5 epitope. As the antibody was raised against the C-terminal domain of Dvl2 (aa 594-736), a series of C-terminal deletion mutants of Dvl2-Myc were generated and analyzed by Western blotting with both Myc antibody and mAb 10B5 (Figure 1B and 1C). The shortest construct that still reacted with both antibodies was Dvl2Δ127, containing amino acids 1-609. Thus, our results placed the epitope within a 16 amino acid sequence from residues 594 to 609 (Figure 1D). This sequence contains two serine and two threonine residues as potential phosphorylation sites, three of which are clustered as STRS at position 594-597. As all three Dvl proteins undergo Wnt-induced phosphorylation and mobility shift (12,34), we examined the equivalent regions of Dvl1 and Dvl3. The STRS motif is perfectly conserved in Dvl1, while the equivalent sequence in Dvl3 is SNRS (Fig. 1D).

To investigate whether in vivo phosphorylation of specific amino acid residues within the 16 aa 10B5 epitope is necessary for the Wnt-induced mobility shift of Dvl2, we individually mutated each of the four Ser and Thr residues to Ala in a Myc-tagged human Dvl2 cDNA and stably expressed the constructs in Rat2 cells by retroviral transduction. Mobility of the mutant proteins was then examined on Western blots of cells treated with or without Wnt3a conditioned medium (CM). No individual Ser/Thr mutation prevented the phosphorylation-dependent mobility shift. However, for each of the mutants S594A and S597A only about 50% of the protein showed slower mobility in response to Wnt3a, indicating that the absence of either of these serines partially impairs formation of psDvl2 (Fig. 2). In contrast, we observed little or no inhibition of psDvl2 formation in T595A or T604A mutants. Apart from the S and T residues, the only other amino acid within the epitope region that is conserved in all three Dvl proteins is R603. When this residue was mutated, Wnt-induced formation of psDvl2 was unaffected, as detected by Myc antibody. However, even in the absence of Wnt treatment, the mutant protein was undetectable by the 10B5 antibody (Fig. 2, lanes 13 and 14). This indicates that R603 is a critical residue in the 10B5 epitope but is unrelated to Wnt-induced phosphorylation.

We next tested combinations of S→A and T→A mutations, again using a retrovirus vector to express Myc-tagged human Dvl2 proteins. Remarkably, mutation of all four Ser/Thr residues (P4m) of the epitope produced a protein that showed no shift in mobility in response to either Wnt3a or Wnt5a signaling (Fig. 3A and 3B). Reagents based on this set of mutations were used in most of the subsequent experiments. For comparison, the Wnt-dependent mobility shift of endogenous Dvl3 was maintained in the cell lines expressing the Dvl2 P4m mutant (Fig. 3A and 3B). We subsequently determined that a mutant, Dvl2 P3m, having alanine substitutions only at S594, T595 and S597, also failed to undergo a Wnt-dependent mobility shift (Fig. 3C). As Dvl2 P3m and P4m are deficient in the Wnt-induced phosphorylation that results in a mobility shift, we refer to them as WIP mutants.

The amino acid sequence of the 10B5 epitope is perfectly conserved between human and mouse Dvl2. To confirm the properties of the Dvl2 P4m WIP mutation in mouse Dvl2, we introduced the same four S→A and T→A changes into a FLAG-tagged mDvl2 cDNA and expressed it in the human Ewing Sarcoma Family Tumor cell line

TC-32 by lentiviral transduction. These cells display significant endogenous Wnt activity, which is associated with a basal level of neurite outgrowth (10). Accordingly, exogenous mDvl2 wild-type (WT) protein was spontaneously phosphorylated and shifted on Western blots (Fig. 3D). However, this shift was abolished by treating the cells for 3 h with the Wnt ligand antagonist sFRP1, consistent with the mobility shift being due to endogenous Wnt production (Fig 3D, lane 3). In contrast, mDvl2 P4m protein showed no phosphorylation-related mobility shift and was unaffected by sFRP1 (Fig. 3D, lanes 4-6). This confirmed that the P4m mutations eliminate the phosphorylation-dependent mobility shift in Dvl2 caused by Wnt signaling.

WIP mutant Dvl2 shows elevated activity in canonical Wnt signaling. The WIP mutant is not only resistant to Wnt-induced phosphorylation at the 10B5 epitope, but it fails to undergo the conformational change that presumably underlies the altered electrophoretic mobility. This mutant is therefore well suited for studying the functional impact of Dvl2 phosphorylation in Wnt signaling.

Although the ability of Wnts to induce Dvl phosphorylation is associated with non-canonical signaling, it also occurs in response to Wnts that concurrently activate the β-catenin pathway (12). To investigate the functional consequences of Dvl phosphorylation in Wnt signaling, we first tested the hypothesis that the Dvl2 WIP mutant might show altered activity in canonical signaling assays. As previously noted (25), transient overexpression of hDvl2 WT in 293T cells gives robust activation of the TCF/β-catenin-dependent luciferase reporter TOPflash in a dose-dependent manner (Fig. 4A). Parallel transfections with the WIP mutant Dvl2 P4m also activated TOPflash. However, at lower doses of input DNA, the signal from hDvl2 P4m was significantly stronger than from hDvl2 WT (Fig. 4A). This suggested that the WIP mutant is moderately hyperactive in β-catenin signaling. We also analyzed cytosolic β-catenin by immunoblotting to compare the responsiveness of these cells to varying Wnt3a concentrations. While a 1:125 dilution of Wnt3a CM elicited only a small accumulation of β-catenin in cells expressing hDvl2 WT, we observed a larger increase in cells expressing hDvl2 P4m (Fig. 4B). Similarly, when mDvl2 WT and P4m constructs were transiently expressed in C57MG mouse mammary epithelial cells, the Wnt3a-dependent induction of β-catenin target genes Axin2 and RhoU (47) was stronger with Dvl2 P4m than Dvl2 WT (Fig. 4C and 4D). Although the differential effects were not dramatic, these experiments suggested that expression of the Dvl2 WIP mutant enhanced the sensitivity of cells to Wnt3a. This implies that Wnt-induced Dvl2 phosphorylation at the identified sites has a modest negative effect on canonical signaling.

WIP mutant Dvl2 preferentially accumulates in puncta. Both endogenous and overexpressed Dvl proteins are known to form cytoplasmic puncta (48,49). These puncta are thought to result from dynamic polymerization of Dvl proteins, and to some extent correlate with activation of Wnt/β-catenin signaling (24-26). When we examined the intracellular distribution of FLAG-tagged mDvl2 WT and mDvl2 P4m stably expressed in TC-32 cells, we observed three different FLAG staining patterns: (1) diffuse cytoplasmic; (2) combination of cytoplasmic and puncta; (3) puncta dominant (Fig. 5A). Quantitative analysis revealed that 64% of cells expressing mDvl2 WT had a diffuse cytoplasmic pattern, 32% had a mixed pattern and 3% were puncta dominant. In contrast, only 15% of cells expressing mDvl2 P4m exhibited a diffuse cytoplasmic distribution, while 78% had a mixed pattern and 6% were puncta dominant (Fig. 5B). Similar profiles were seen in the presence and absence of Wnt3a treatment with or without siRNA knockdown of endogenous Dvl2/3 expression (data not shown). The enhanced accumulation of P4m in puncta is consistent with its stimulation of β-catenin signaling.

WIP mutant Dvl2 does not mediate Wnt3a-dependent neurite outgrowth in TC-32 cells. Wnt3a induces neurite outgrowth in TC-32 cells via non-canonical Wnt signaling, and Dvl proteins are required for this process (10). Moreover, a Wnt3a-dependent Dvl mobility shift correlates with neurite outgrowth in these cells (43). Using this experimental model as a readout for non-canonical Wnt signaling, we compared the ability of siRNA-resistant mDvl2 WT vs. P4m proteins to rescue Wnt-induced neurite outgrowth after knockdown of endogenous Dvl2/3. Dvl2/3 siRNA markedly blocked Wnt-3a-dependent neurite outgrowth in parental TC-32 cells (Fig. 6A). However, neurite extension was not inhibited in cells expressing mDvl2 WT. In contrast, mDvl2

P4m failed to rescue neurite outgrowth. Moreover, expression of P4m also blocked Wnt3a-induced neurite outgrowth in the presence of endogenous Dvl2/3 (Fig. 6A). mDvl2 WT and P4m proteins were expressed at similar levels and knockdown of endogenous Dvl2/3 proteins was comparable in the various cell lines, indicating that differences in expression did not account for their distinct effects (Fig. 6B). Interestingly, levels of both FLAG-tagged Dvl2 WT and P4m were significantly increased, and to a similar extent, after siRNA knockdown of endogenous Dvl2/3 (Fig. 6B). Nonetheless, the results from these experiments clearly demonstrate that the Dvl2 WIP mutant was unable to support neurite outgrowth, implying that it was defective in mediating the requisite non-canonical Wnt signaling.

CK1δ phosphorylates CTD residues responsible for the WIP-dependent mobility shift. Previous studies have demonstrated that knockdown of endogenous CK1δ and CK1ε with small interfering RNA blocks the Wnt-dependent psDvl mobility shift (39,43). We therefore performed an *in vitro* kinase assay with purified CK1δ and hDvl2, followed by tryptic digestion and mass spectrometry analysis, to determine whether the residues implicated in the mobility shift were targets of CK1 phosphorylation. While several phosphorylation sites were detected elsewhere in the hDvl2 sequence (unpublished observations, KHL), we recovered multiple phosphopeptides with phosphorylation at residues S594, T596, and S597, but not T604 (Table 1). In addition, S591 and S592 were phosphorylated. Thus, each of the amino acid residues S594, T595 and S597 conforms to the consensus CK1 phosphorylation site pS/pT–X_{1-3}–S/T, where underlined residues are the target sites. As previously noted, a Dvl2 triple mutant with alanine substitutions at these residues (P3m) did not undergo a mobility shift following Wnt3a treatment (Fig. 3C). Taken together, our data indicate that the Wnt-dependent psDvl2 mobility shift is due to CK1δ/ε phosphorylation of these three residues.

DISCUSSION

In this study we have identified Wnt-induced phosphorylation (WIP) sites at Ser594, Thr595, and Ser597 in Dvl2 that have functional consequences for both canonical and non-canonical signaling. These sites have particular significance among other phosphorylation sites that have been mapped on Dvl proteins in the past. First, phosphorylation of the WIP sites is induced by Wnt ligand signaling rather than by overexpression of individual kinases. Second, the phosphorylation of these sites is required for the Wnt-mediated Dvl2 electrophoretic mobility shift that is routinely used as an assay for Dvl phosphorylation, and also serves as an assay for non-canonical Wnt signal transduction events (12,20). Although two amino acids in the DIX domain of Dvl2, K68 and E69, were previously shown to be required for formation of psDvl2, these residues are not phosphorylated but instead affect subcellular Dvl2 distribution (50).

Several previous studies have implied that CK1δ and CK1ε are primarily responsible for the Wnt-dependent mobility shift of Dvl2/3(30,39,43). Consistent with this notion, we found that the WIP sites identified here were phosphorylated by CK1δ in an *in vitro* kinase assay. Others have documented CK1 phosphorylation sites elsewhere in Dvl protein (36) and we also detected phosphorylation of other residues in our *in vitro* kinase assay (data not shown). In view of the abundance of potential phosphorylation targets throughout the Dvl2 amino acid sequence, therefore, the abolition of mobility shifting by mutation of these three residues alone is perhaps unexpected. However, we suggest that phosphorylation of the WIP sites may be a necessary priming event that allows further phosphorylation at other sites, and/or that WIP site phosphorylation in conjunction with other phosphorylated sites creates a critical mass of charged residues sufficient to bring about the presumed conformational change in Dvl protein that causes its electrophoretic retardation. In this regard it is notable that, in overexpression experiments, CK1δ and CK1ε can induce phosphorylation at sites in Dvl2 other than the WIP sites and that this in turn can cause mobility shifting (data not shown). A similar finding was recently reported for a Dvl3 CTD deletion mutant (39). Nevertheless, our results demonstrate that when Dvl phosphorylation is triggered by Wnt ligands, mutation of the WIP sites prevents mobility shifting in cells expressing endogenous levels of CK1δ/ε. Thus, these sites are likely to have physiologic relevance.

Mutation of the WIP sites of Dvl2 provided a unique opportunity to investigate the functional consequences of preventing Wnt-induced phosphorylation of mammalian Dvl without alterations in the activity of kinases that might have pleiotropic effects. To some extent our conclusions differ from an extensive analysis of Dishevelled (Dsh) phosphorylation in *Drosophila*, which concluded that Ser/Thr phosphorylation did not have functional significance in β-catenin or PCP signaling (35). However, the authors of that study acknowledged the possibility that phosphorylation of mammalian Dvls at residues not conserved in *Drosophila* might be functionally relevant, especially in pathways that were not operative in their assays. These caveats apply to the $S^{594}T^{595}R^{596}S^{597}$ sequence we identified in Dvl2, as it is located in a region poorly conserved in *Drosophila* but well conserved in mammals and other vertebrates (51).

Our functional testing of Dvl2 WIP mutants suggests that phosphorylation of these three Ser/Thr residues has a mild inhibitory effect on canonical Wnt/β-catenin signaling, as the alanine substitution mutant Dvl2 P4m appeared more active than Dvl2 WT in assays of β-catenin-mediated transcription. More strikingly, and in contrast, Dvl2 P4m was unable to rescue Wnt3a-induced neurite outgrowth in TC-32 cells. We have previously reported that Wnt-mediated neurite extension in these cells does not require the canonical Wnt/β-catenin pathway receptor LRP5/6 and instead is mediated by non-canonical Wnt pathways that rely on JNK and atypical PKC iota (PKCι) (10)(Greer et al., submitted). In the accompanying manuscript we further show that Dvl2 P4m, in contrast to Dvl2 WT, fails to co-immunoprecipitate with PKCι and this may account for its inability to mediate neurite outgrowth (Greer et al., submitted). The inactivity of Dvl2 P4m in the neurite assay indicates that it cannot transduce an essential non-canonical signal and hence that phosphorylation of the Dvl2 WIP sites normally promotes this function.

In apparent contrast to our results concerning the impact of Wnt-induced, CK1δ/ε-dependent Dvl2 phosphorylation on β-catenin signaling, a number of previous studies have implicated CK1δ/ε as a positive mediator of the canonical pathway (52,53). One explanation of this may stem from the ability of overexpressed CK1δ/ε to phosphorylate several other Wnt signaling components besides Dvl and thus to exert a combination of positive and negative effects on the pathway as a whole (40). In addition, there appear to be differential effects of CK1-mediated phosphorylation at different sites within Dvl proteins. For example, a recent report indicated that CK1ε phosphorylation of Dvl3 at upstream sites correlated with stimulation of canonical signaling, while phosphorylation in the CTD was associated with attenuation of the signal (39). The consequences we describe here for phosphorylation of the WIP sites in the CTD of Dvl2 are consistent with that report.

We also examined the effect of WIP site mutation on subcellular distribution of Dvl2 protein, especially with regard to formation of the cytoplasmic puncta that are associated with Wnt/β-catenin signaling (24,25,27,50). Our observation that Dvl2 P4m preferentially localized to puncta relative to Dvl2 WT (Fig. 5) is consistent with this view, as the mutant was more potent in assays of canonical Wnt/β-catenin signaling. Our findings are also in agreement with those of Bernatik et al. (39) who noted increased localization in puncta of a ps-deficient Dvl3 deletion derivative that showed enhanced activity in the β-catenin pathway. The results from these studies together reinforce the idea that phosphorylation in the CTD is associated with diminished β-catenin signaling. Others have not specifically addressed the possibility that phosphorylation of the CTD would have a positive effect on other Dvl activities, and this is an important additional conclusion from our study. Phosphorylation at the CTD WIP sites might therefore serve as a switch to redirect Dvl function towards non-canonical signaling. This may have particular relevance for Wnt ligands that can stimulate both canonical and non-canonical pathways (12). In view of the 20-30 minute time lag before induction of psDvl2, there may be attenuation of canonical signaling over time via this mechanism.

REFERENCES

1. Klingensmith, J., Nusse, R., and Perrimon, N. (1994) The Drosophila segment polarity gene dishevelled encodes a novel protein required for response to the wingless signal. *Genes Dev* **8**, 118-130
2. Sussman, D. J., Klingensmith, J., Salinas, P., Adams, P. S., Nusse, R., and Perrimon, N. (1994) Isolation and characterization of a mouse homolog of the *Drosophila* segment polarity gene *dishevelled*. *Devl.Biol.* **166**, 73-86
3. Gao, C., and Chen, Y. G. (2010) Dishevelled: The hub of Wnt signaling. *Cell Signal* **22**, 717-727
4. Klaus, A., and Birchmeier, W. (2008) Wnt signalling and its impact on development and cancer. *Nat Rev Cancer* **8**, 387-398
5. Clevers, H. (2006) Wnt/beta-catenin signaling in development and disease. *Cell* **127**, 469-480
6. Veeman, M. T., Axelrod, J. D., and Moon, R. T. (2003) A second canon. Functions and mechanisms of beta-catenin-independent Wnt signaling. *Dev Cell* **5**, 367-377
7. MacDonald, B. T., Tamai, K., and He, X. (2009) Wnt/beta-catenin signaling: components, mechanisms, and diseases. *Dev Cell* **17**, 9-26
8. Shimizu, H., Julius, M. A., Giarre, M., Zheng, Z., Brown, A. M., and Kitajewski, J. (1997) Transformation by Wnt family proteins correlates with regulation of beta-catenin. *Cell Growth Differ* **8**, 1349-1358
9. Endo, Y., Wolf, V., Muraiso, K., Kamijo, K., Soon, L., Uren, A., Barshishat-Kupper, M., and Rubin, J. S. (2005) Wnt-3a-dependent cell motility involves RhoA activation and is specifically regulated by dishevelled-2. *J Biol Chem* **280**, 777-786
10. Endo, Y., Beauchamp, E., Woods, D., Taylor, W. G., Toretsky, J. A., Uren, A., and Rubin, J. S. (2008) Wnt-3a and Dickkopf-1 stimulate neurite outgrowth in Ewing tumor cells via a Frizzled3- and c-Jun N-terminal kinase-dependent mechanism. *Mol Cell Biol* **28**, 2368-2379
11. Habas, R., Kato, Y., and He, X. (2001) Wnt/Frizzled activation of Rho regulates vertebrate gastrulation and requires a novel Formin homology protein Daam1. *Cell* **107**, 843-854
12. González-Sancho, J. M., Brennan, K. R., Castelo-Soccio, L. A., and Brown, A. M. C. (2004) Wnt proteins induce dishevelled phosphorylation via an LRP5/6- independent mechanism, irrespective of their ability to stabilize beta-catenin. *Mol Cell Biol* **24**, 4757-4768
13. Seifert, J. R., and Mlodzik, M. (2007) Frizzled/PCP signalling: a conserved mechanism regulating cell polarity and directed motility. *Nat Rev Genet* **8**, 126-138
14. O'Connell, M. P., Fiori, J. L., Xu, M., Carter, A. D., Frank, B. P., Camilli, T. C., French, A. D., Dissanayake, S. K., Indig, F. E., Bernier, M., Taub, D. D., Hewitt, S. M., and Weeraratna, A. T. (2010) The orphan tyrosine kinase receptor, ROR2, mediates Wnt5A signaling in metastatic melanoma. *Oncogene* **29**, 34-44
15. Enomoto, M., Hayakawa, S., Itsukushima, S., Ren, D. Y., Matsuo, M., Tamada, K., Oneyama, C., Okada, M., Takumi, T., Nishita, M., and Minami, Y. (2009) Autonomous regulation of osteosarcoma cell invasiveness by Wnt5a/Ror2 signaling. *Oncogene* **28**, 3197-3208
16. Kikuchi, A., and Yamamoto, H. (2008) Tumor formation due to abnormalities in the beta-catenin-independent pathway of Wnt signaling. *Cancer Sci* **99**, 202-208

17. McDonald, S. L., and Silver, A. (2009) The opposing roles of Wnt-5a in cancer. *Br J Cancer* **101**, 209-214
18. Nishita, M., Enomoto, M., Yamagata, K., and Minami, Y. (2010) Cell/tissue-tropic functions of Wnt5a signaling in normal and cancer cells. *Trends Cell Biol* **20**, 346-354
19. James, R. G., Conrad, W. H., and Moon, R. T. (2008) Beta-catenin-independent Wnt pathways: signals, core proteins, and effectors. *Methods Mol Biol* **468**, 131-144
20. Ho, H. Y., Susman, M. W., Bikoff, J. B., Ryu, Y. K., Jonas, A. M., Hu, L., Kuruvilla, R., and Greenberg, M. E. (2012) Wnt5a-Ror-Dishevelled signaling constitutes a core developmental pathway that controls tissue morphogenesis. *Proc Natl Acad Sci U S A* **109**, 4044-4051
21. Kikuchi, A., Yamamoto, H., Sato, A., and Matsumoto, S. (2011) New insights into the mechanism of Wnt signaling pathway activation. *Int Rev Cell Mol Biol* **291**, 21-71
22. Semenov, M. V., Habas, R., Macdonald, B. T., and He, X. (2007) SnapShot: Noncanonical Wnt Signaling Pathways. *Cell* **131**, 1378
23. Wharton, K. A., Jr. (2003) Runnin' with the Dvl: proteins that associate with Dsh/Dvl and their significance to Wnt signal transduction. *Dev Biol* **253**, 1-17.
24. Schwarz-Romond, T., Merrifield, C., Nichols, B. J., and Bienz, M. (2005) The Wnt signalling effector Dishevelled forms dynamic protein assemblies rather than stable associations with cytoplasmic vesicles. *J Cell Sci* **118**, 5269-5277
25. Schwarz-Romond, T., Metcalfe, C., and Bienz, M. (2007) Dynamic recruitment of axin by Dishevelled protein assemblies. *J Cell Sci* **120**, 2402-2412
26. Schwarz-Romond, T., Fiedler, M., Shibata, N., Butler, P. J., Kikuchi, A., Higuchi, Y., and Bienz, M. (2007) The DIX domain of Dishevelled confers Wnt signaling by dynamic polymerization. *Nat Struct Mol Biol* **14**, 484-492
27. Bilic, J., Huang, Y. L., Davidson, G., Zimmermann, T., Cruciat, C. M., Bienz, M., and Niehrs, C. (2007) Wnt induces LRP6 signalosomes and promotes dishevelled-dependent LRP6 phosphorylation. *Science* **316**, 1619-1622
28. Taelman, V. F., Dobrowolski, R., Plouhinec, J. L., Fuentealba, L. C., Vorwald, P. P., Gumper, I., Sabatini, D. D., and De Robertis, E. M. (2010) Wnt signaling requires sequestration of glycogen synthase kinase 3 inside multivesicular endosomes. *Cell* **143**, 1136-1148
29. Lee, J. S., Ishimoto, A., and Yanagawa, S. (1999) Characterization of mouse dishevelled (Dvl) proteins in Wnt/Wingless signaling pathway. *J Biol Chem* **274**, 21464-21470
30. Bryja, V., Schulte, G., Rawal, N., Grahn, A., and Arenas, E. (2007) Wnt-5a induces Dishevelled phosphorylation and dopaminergic differentiation via a CK1-dependent mechanism. *J Cell Sci* **120**, 586-595
31. Van Leeuwen, F., Samos, C. H., and Nusse, R. (1994) Biological activity of soluble *wingless* protein in cultured *Drosophila* imaginal disc cells. *Nature* **368**, 342-344
32. Lee, E., Salic, A., and Kirschner, M. W. (2001) Physiological regulation of beta-catenin stability by Tcf3 and CK1epsilon. *J Cell Biol* **154**, 983-993.
33. Schulte, G., Bryja, V., Rawal, N., Castelo-Branco, G., Sousa, K. M., and Arenas, E. (2005) Purified Wnt-5a increases differentiation of midbrain dopaminergic cells and dishevelled phosphorylation. *J Neurochem* **92**, 1550-1553
34. Bryja, V., Schulte, G., and Arenas, E. (2007) Wnt-3a utilizes a novel low dose and rapid pathway that does not require casein kinase 1-mediated phosphorylation of Dvl to activate beta-catenin. *Cell Signal* **19**, 610-616

35. Yanfeng, W. A., Berhane, H., Mola, M., Singh, J., Jenny, A., and Mlodzik, M. (2011) Functional dissection of phosphorylation of Disheveled in Drosophila. *Dev Biol* **360**, 132-142
36. Klimowski, L. K., Garcia, B. A., Shabanowitz, J., Hunt, D. F., and Virshup, D. M. (2006) Site-specific casein kinase 1epsilon-dependent phosphorylation of Dishevelled modulates beta-catenin signaling. *FEBS J* **273**, 4594-4602
37. Elbert, M., Cohen, D., and Musch, A. (2006) PAR1b promotes cell-cell adhesion and inhibits dishevelled-mediated transformation of Madin-Darby canine kidney cells. *Mol Biol Cell* **17**, 3345-3355
38. Kikuchi, K., Niikura, Y., Kitagawa, K., and Kikuchi, A. (2010) Dishevelled, a Wnt signalling component, is involved in mitotic progression in cooperation with Plk1. *EMBO J* **29**, 3470-3483
39. Bernatik, O., Ganji, R. S., Dijksterhuis, J. P., Konik, P., Cervenka, I., Polonio, T., Krejci, P., Schulte, G., and Bryja, V. (2011) Sequential activation and inactivation of Dishevelled in the Wnt/beta-catenin pathway by casein kinases. *J Biol Chem* **286**, 10396-10410
40. Knippschild, U., Gocht, A., Wolff, S., Huber, N., Lohler, J., and Stoter, M. (2005) The casein kinase 1 family: participation in multiple cellular processes in eukaryotes. *Cell Signal* **17**, 675-689
41. Liu, C., Li, Y., Semenov, M., Han, C., Baeg, G. H., Tan, Y., Zhang, Z., Lin, X., and He, X. (2002) Control of beta-catenin phosphorylation/degradation by a dual-kinase mechanism. *Cell* **108**, 837-847
42. Uren, A., Reichsman, F., Anest, V., Taylor, W. G., Muraiso, K., Bottaro, D. P., Cumberledge, S., and Rubin, J. S. (2000) Secreted frizzled-related protein-1 binds directly to Wingless and is a biphasic modulator of Wnt signaling. *J Biol Chem* **275**, 4374-4382
43. Greer, Y. E., and Rubin, J. S. (2011) Casein kinase 1 delta functions at the centrosome to mediate Wnt-3a-dependent neurite outgrowth. *J Cell Biol* **192**, 993-1004
44. Brown, A. M. C., and Dougherty, J. P. (1995) Retroviral vectors. in *DNA Cloning IV, Mammalian Systems - A Practical Approach* (Glover, D. M., and Hames, B. D. eds.), Oxford University Press, Oxford. pp 113-142
45. Brennan, K., González-Sancho, J. M., Castelo-Soccio, L. A., Howe, L. R., and Brown, A. M. C. (2004) Truncated mutants of the putative Wnt receptor LRP6/Arrow can stabilize beta-catenin independently of Frizzled proteins. *Oncogene* **23**, 4873-4884
46. Howe, L. R., Crawford, H. C., Subbaramaiah, K., Hassell, J. A., Dannenberg, A. J., and Brown, A. M. C. (2001) PEA3 is up-regulated in response to Wnt1 and activates the expression of cyclooxygenase-2. *J Biol Chem* **276**, 20108-20115.
47. Baljinnyam, B., Klauzinska, M., Saffo, S., Callahan, R., and Rubin, J. S. (2012) Recombinant R-spondin2 and Wnt3a up- and down-regulate novel target genes in C57MG mouse mammary epithelial cells. *PLoS One* **7**, e29455
48. Yanagawa, S., van Leeuwen, F., Wodarz, A., Klingensmith, J., and Nusse, R. (1995) The dishevelled protein is modified by wingless signaling in Drosophila. *Genes Dev* **9**, 1087-1097
49. Yang-Snyder, J., Miller, J. R., Brown, J. D., Lai, C. J., and Moon, R. T. (1996) A frizzled homolog functions in a vertebrate Wnt signaling pathway. *Curr Biol* **6**, 1302-1306

50. Capelluto, D. G., Kutateladze, T. G., Habas, R., Finkielstein, C. V., He, X., and Overduin, M. (2002) The DIX domain targets dishevelled to actin stress fibres and vesicular membranes. *Nature* **419**, 726-729
51. Semenov, M. V., and Snyder, M. (1997) Human dishevelled genes constitute a DHR-containing multigene family. *Genomics* **42**, 302-310
52. Peters, J. M., McKay, R. M., McKay, J. P., and Graff, J. M. (1999) Casein kinase I transduces Wnt signals. *Nature* **401**, 345-350
53. Sakanaka, C., Leong, P., Xu, L., Harrison, S. D., and Williams, L. T. (1999) Casein kinase iepsilon in the wnt pathway: regulation of beta-catenin function. *Proc Natl Acad Sci U S A* **96**, 12548-12552

Acknowledgements - We are grateful to Keith Brennan, Brittany Carson, Louise Howe, Keiji Itoh and Sergei Sokol for fruitful discussions, and to Tamara Weissman for technical support. We thank Xi He, Sean Lee and David Virshup for providing plasmid reagents. This work was supported by the National Institutes of Health (R01 CA123238 to A.M.C.B.), a fellowship from the Ministerio de Educación, Cultura, y Deportes, of Spain (to J.M.G.-S.), NIH postdoctoral fellowship F32 CA117662 to C.A.A., New York State Department of Health postdoctoral fellowship NYS C021339 to Y.T., and by charitable donations to Strang Cancer Prevention Center. This research also was supported, in part, by the Intramural Research Program of the National Institutes of Health, National Cancer Institute.

FIGURE LEGENDS

Fig. 1. **Deletion mapping of Wnt-induced phosphorylation sites in Dvl2 associated with mobility shift and mAb 10B5 epitope recognition.** (A) Immunoblots showing Wnt-induced mobility shift of endogenous (left panels) and exogenous (right panels) Dvl2 proteins, and the inability of mAb 10B5 to detect the mobility shifted forms. Rat2 fibroblasts transduced with control retroviral vector (left panels), or vector expressing Myc-tagged hDvl2 (right panels), were treated with Wnt3a conditioned medium (CM) for 2 h and lysates were processed for western analysis with the indicated antibodies. Bands corresponding to hypophosphorylated (Dvl2) or phosphorylated and shifted Dvl2 (psDvl2) are indicated. The expected locations of psDvl and ps-hDvl2-Myc are indicated in the lower panels but the bands are undetectable with mAb 10B5. (B) Schematic diagram of Dvl2 C-terminal deletion mutants. Sequences of full-length hDvl2 (1-736 residues) and truncated derivatives are represented, along with positions of the modular domains, DIX, b (basic region), PDZ, and DEP. Sequences present in the immunogen for MAb 10B5 (594-736) are indicated in grey. (C) Immunoblots of Myc-tagged hDvl2 full-length and deletion constructs transiently transfected in HEK293T cells. Proteins were detected with mAb 10B5 or anti-Myc. Molecular mass markers are indicated. (D) Sequence comparison of human Dvl isoforms in region corresponding to deduced 10B5 epitope. Extent of epitope is demarcated by the box. Potential Ser/Thr phosphorylation sites within epitope are highlighted in black. Epitope residues conserved in all 3 Dvl proteins are designated with *.

Fig. 2. **Site-directed mutagenesis identified individual residues that contribute to Dvl2 mobility shift.** Each of the S/T residues and conserved R603 in the putative epitope of the Dvl2 mAb 10B5 were mutated as indicated and Myc-tagged hDvl2 derivatives were stably expressed in Rat2 cells by retroviral transduction. After incubation for 2 h with Wnt3a CM or control CM,

cell lysates were analyzed by immunoblotting with anti-Myc and Dvl2 10B5 antibodies. Bands corresponding to endogenous and exogenous Dvl2 and psDvl2 are indicated.

Fig. 3. **Wnt-dependent mobility shift of Dvl2 WT vs. P4m and P3m mutants.** Western blot analysis of Rat2 cells stably transduced with Myc-tagged hDvl2 WT, hDvl2 P4m or empty retroviral vector and incubated overnight with Wnt3a CM (A) or Wnt5a CM (B). Exogenous Myc-tagged Dvl2 was detected with anti-Myc (upper panels). Dvl3 was probed for comparison (lower panels), providing a positive control for Wnt-induced phosphorylation of endogenous Dvl, and GSK3β served as a loading control. (C) A similar analysis was performed with Rat2 cells stably expressing Myc-tagged hDvl2 WT, P4m or P3m and treated with Wnt3a CM. (D) Immunoblot of FLAG-tagged mDvl2 WT and 4Pm in TC-32 cells with or without sFRP1 treatment. HSP70 served as a loaded control.

Fig. 4. **WIP mutant exhibits greater activity than hDvl2 WT in the β-catenin pathway.** (A) Topflash reporter assay in 293T cells. Cells were transiently transfected with Topflash reporter and empty vector (negative control), β-catenin cDNA (positive control), or varying amounts of hDvl2 WT or hDvl2 P4m expression constructs. Results were normalized to activity obtained with empty vector (50 ng/well). (B) β-catenin stabilization in Rat2 cells stably transduced with hDvl2 WT or P4m vectors. Cells were treated with the indicated dilutions of Wnt3a CM and lysates were blotted for β-catenin and GSK-3β; the latter was a loading control. At low doses of Wnt3a, cells expressing P4m were more sensitive to β-catenin stablization than those expressing hDvl2 WT. The experiment was performed twice with similar results. (C and D) C57MG cells were transiently transfected with empty vector, FLAG-tagged mDvl2 WT or P4m constructs and subsequently incubated with or without Wnt3a (50 ng/ml) for 6 h. Quantitative RT-PCR analysis of Axin2 (C) and RhoU transcripts (D) was normalized to β-actin transcript and expressed in arbitrary units with 1 unit = expression in cells transfected with empty vector and incubated in the absence of Wnt3a. Results are the mean of triplicate measurements $\pm$ S.D. from one of two experiments that yielded similar data.

Fig. 5. **Intracellular distribution of FLAG-tagged mDvl2 WT and mDvl2 P4m in TC-32 cells.** (A) Representative micrographs of FLAG-mDvl2 distribution illustrating three patterns: cytoplasmic; cytoplasmic and puncta; puncta predominant. (B) Cumulative quantitative analysis of distribution patterns for mDvl2 WT and P4m. N indicates the number of cells examined for each construct.

Fig. 6. **Contrasting activity of FLAG-tagged mDvl2 WT vs. mDvl2 P4m in neurite outgrowth assay.** (A) Parental TC-32 cells and cells stably expressing FLAG-tagged mDvl2 WT or mDvl2 P4m were treated with siRNA reagents targeting luciferase (negative control) or Dvl2 and Dvl3, and 48 h later incubated with medium +/- Wnt3a (100 ng/ml) for 3 h. Following fixation, neurite outgrowth was assessed in dozens of cells from each treatment group. The results from three separate experiments are indicated, mean and S.D. Statistical significance of selected pairwise comparisons is indicated. (B) Western blot analysis of Dvl2/3 expression in cells treated as described in (A). Efficacy of Dvl2/3 siRNA is evident. HSP70 was a loading control. Position of molecular mass markers is indicated.

In vitro kinase reaction	Peptides identified	Phosphosites	Region
CK1δ + Dvl2	R.SSG**S**TRSDGGAGR.T	S591, **S594**	590 - 604
	R.SSGS**T**RSDGGAGR.T	S591, **T595**	
	R.SSG**S**TR**S**DGGAGR.T	S592, **S594**, **S597**	
	R.SSGS**T**R**S**DGGAGR.T	S591, **T595**, **S597**	

Table 1. Phosphopeptides derived from region 590-604 of hDvl2 after in vitro phosphorylation with CK1δ, detected by mass spectrometry. Dots indicate sites of tryptic cleavage. Underlines indicate phosphorylated residues. Boldface indicates phosphorylated residues implicated in psDvl2 mobility shift and 10B5 epitope.

Figure 1

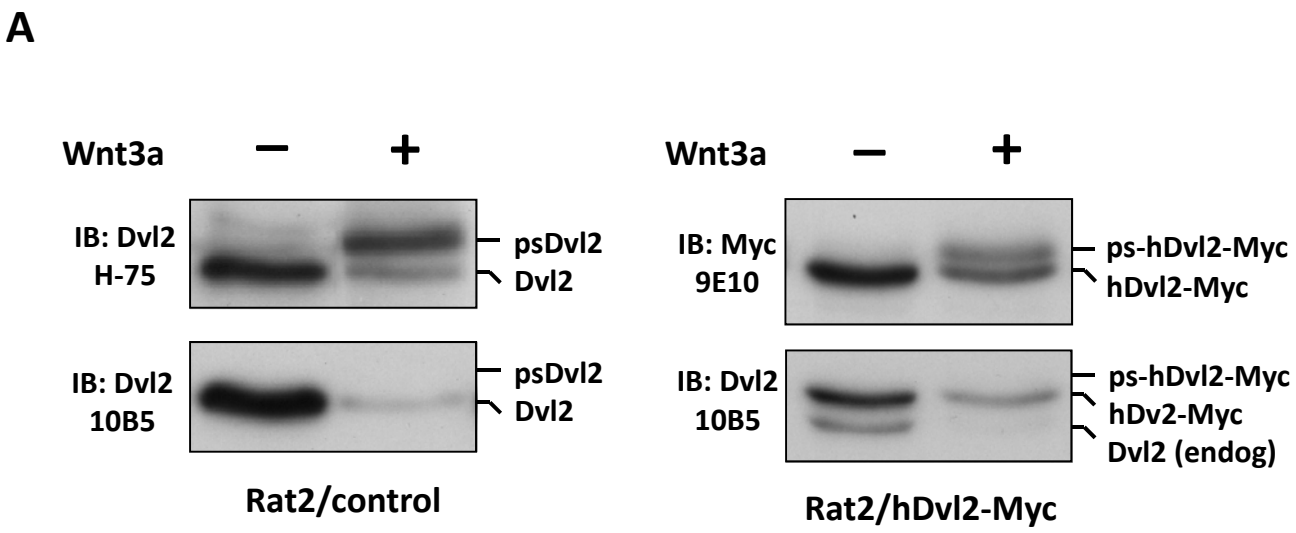
A
Wnt3a
–
+
IB: Dvl2
H-75
psDvl2
Dvl2
IB: Dvl2
10B5
psDvl2
Dvl2
Rat2/control
Wnt3a
–
+
IB: Myc
9E10
ps-hDvl2-Myc
hDvl2-Myc
IB: Dvl2
10B5
ps-hDvl2-Myc
hDv2-Myc
Dvl2 (endog)
Rat2/hDvl2-Myc

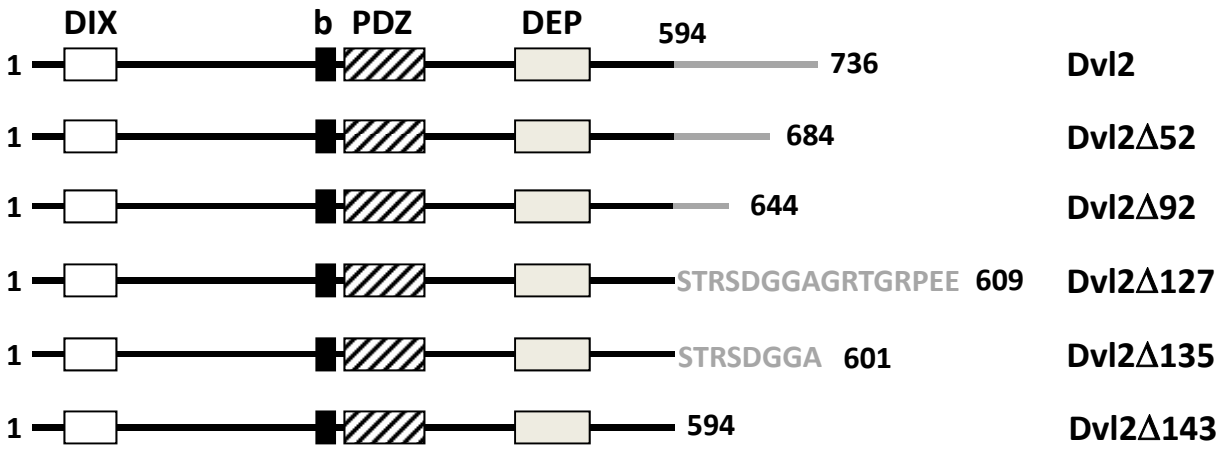
B
DIX
b
PDZ
DEP
594
1
736
Dvl2
1
684
Dvl2Δ52
1
644
Dvl2Δ92
1
STRSDGGAGRTGRPEE
609
Dvl2Δ127
1
STRSDGGA
601
Dvl2Δ135
1
594
Dvl2Δ143

Figure 1

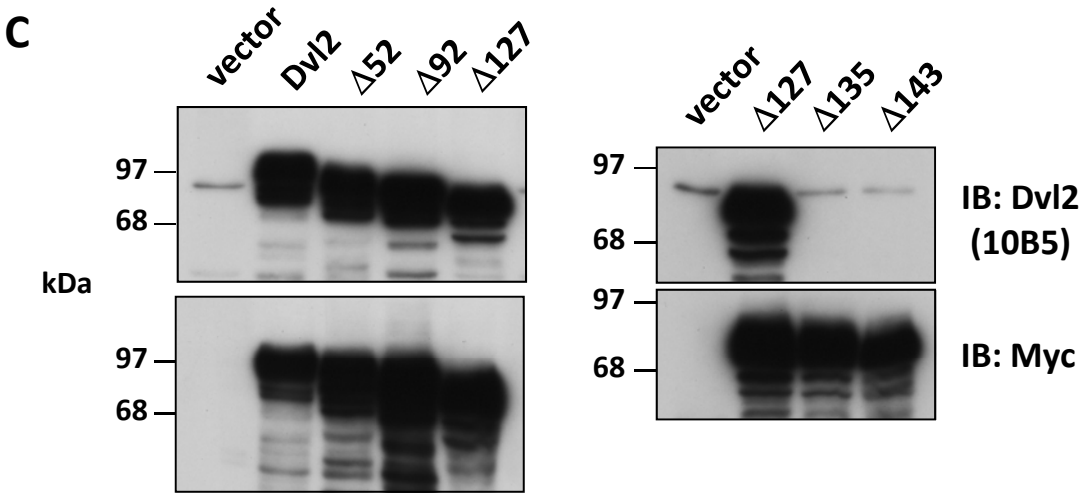

D

	594	595	597	603	604	609
hDvl2	SEGSRSSG	**S**	T	R	**S**	DGGAGR**T**GRPEERAP
hDvl1	SEGSKSSG	**S**	T	R	**S**	---SRRAPGREKERR
hDvl3	SEGSRSSG	**S**	N	R	**S**	--GSDRRKEKDPKAG
		*	**			*

Figure 2

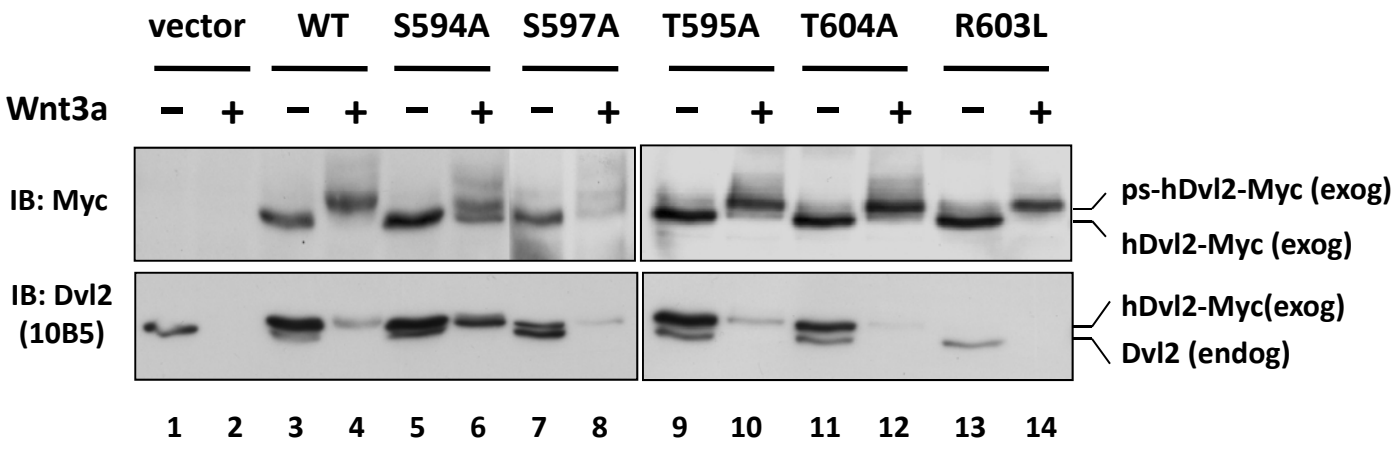
vector
WT
S594A
S597A
T595A
T604A
R603L
Wnt3a
– + – + – + – + – + – + – +
IB: Myc
IB: Dvl2 (10B5)
ps-hDvl2-Myc (exog)
hDvl2-Myc (exog)
hDvl2-Myc(exog)
Dvl2 (endog)
1 2 3 4 5 6 7 8 9 10 11 12 13 14

Figure 3

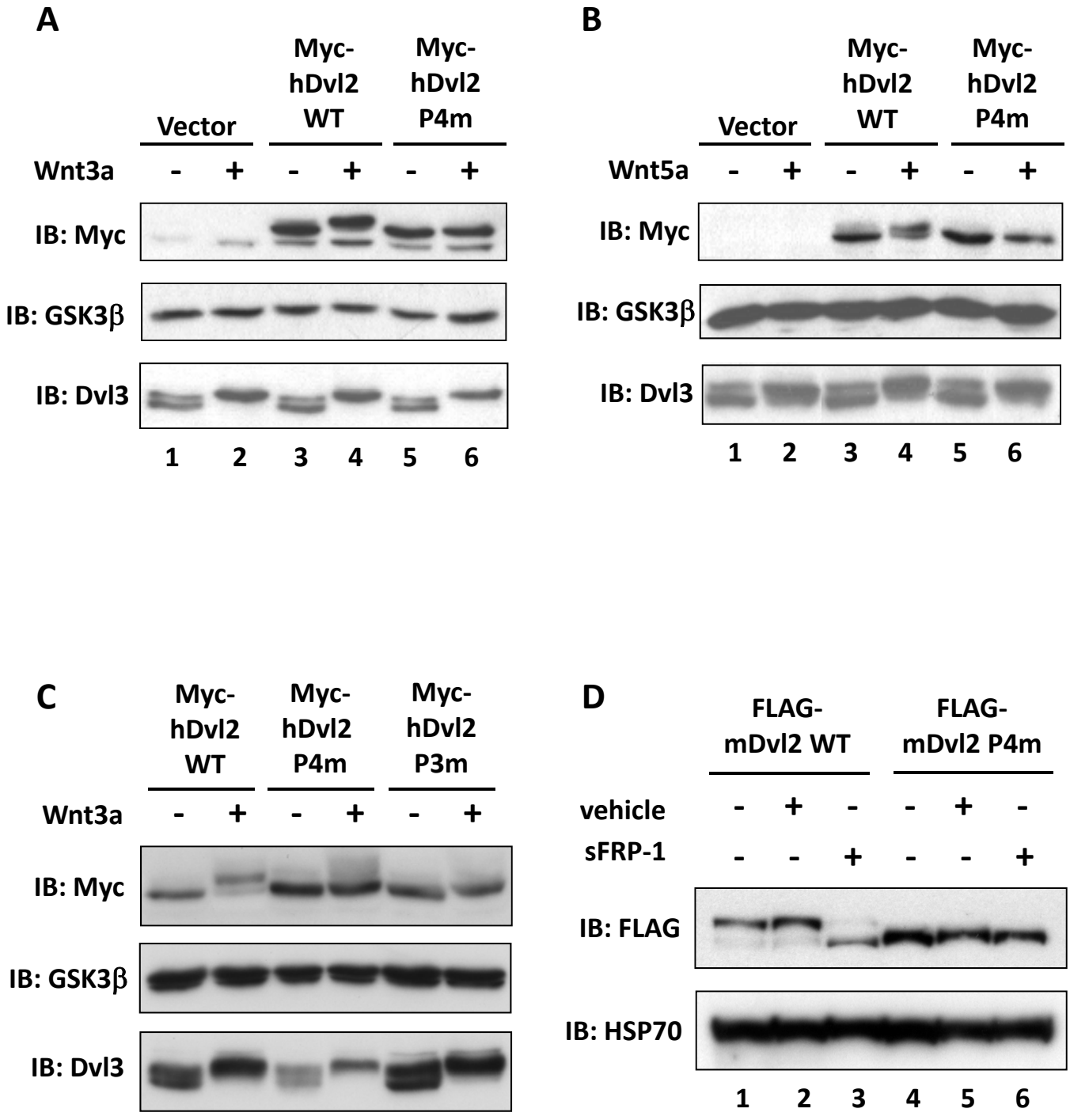
A
Vector
Myc-hDvl2 WT
Myc-hDvl2 P4m
Wnt3a
- + - + - +
IB: Myc
IB: GSK3β
IB: Dvl3
1 2 3 4 5 6
B
Vector
Myc-hDvl2 WT
Myc-hDvl2 P4m
Wnt5a
- + - + - +
IB: Myc
IB: GSK3β
IB: Dvl3
1 2 3 4 5 6
C
Myc-hDvl2 WT
Myc-hDvl2 P4m
Myc-hDvl2 P3m
Wnt3a
- + - + - +
IB: Myc
IB: GSK3β
IB: Dvl3
D
FLAG-mDvl2 WT
FLAG-mDvl2 P4m
vehicle
- + - - + -
sFRP-1
- - + - - +
IB: FLAG
IB: HSP70
1 2 3 4 5 6

Figure 4

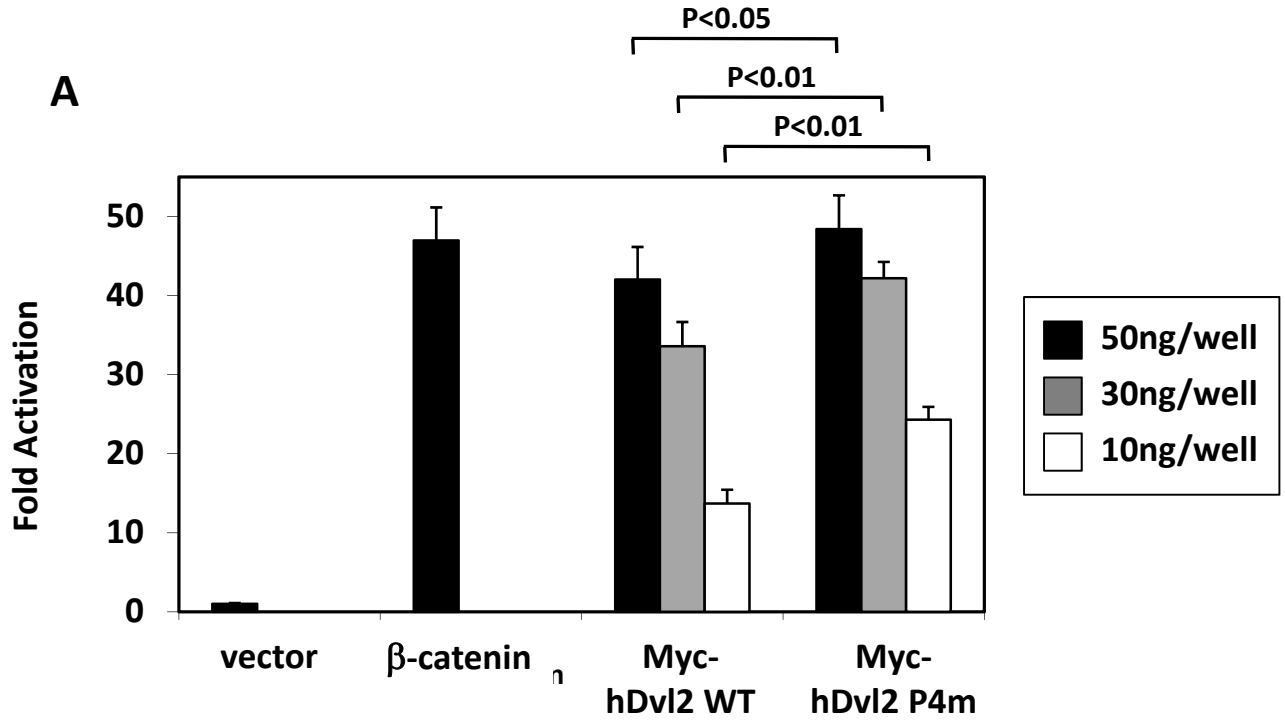
A
P<0.05
P<0.01
P<0.01
Fold Activation
50
40
30
20
10
0
vector
β-catenin
Myc-hDvl2 WT
Myc-hDvl2 P4m
50ng/well
30ng/well
10ng/well

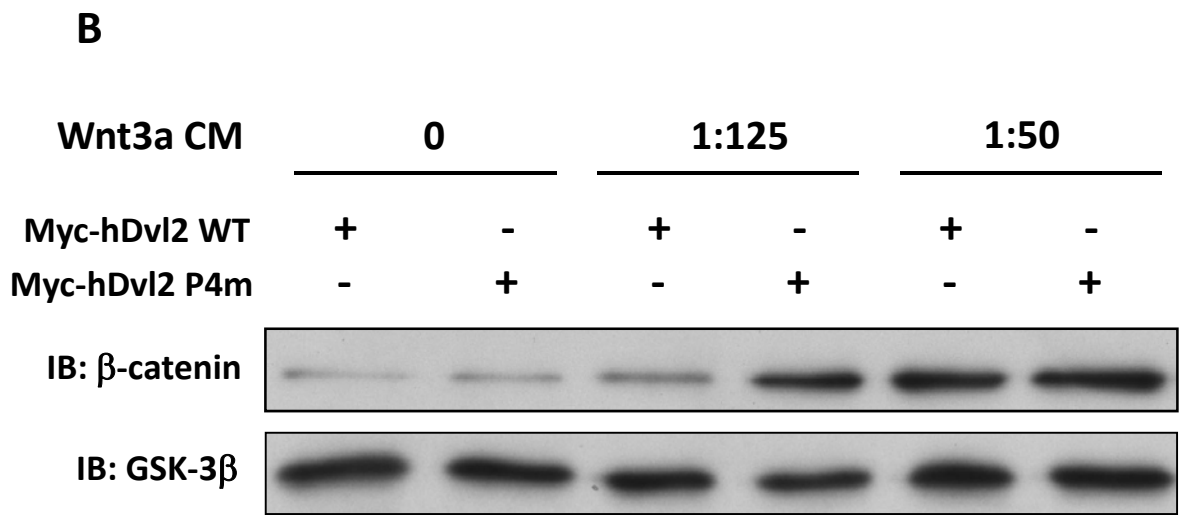
B
Wnt3a CM
0
1:125
1:50
Myc-hDvl2 WT
+ - + - + -
Myc-hDvl2 P4m
- + - + - +
IB: β-catenin
IB: GSK-3β

Figure 4

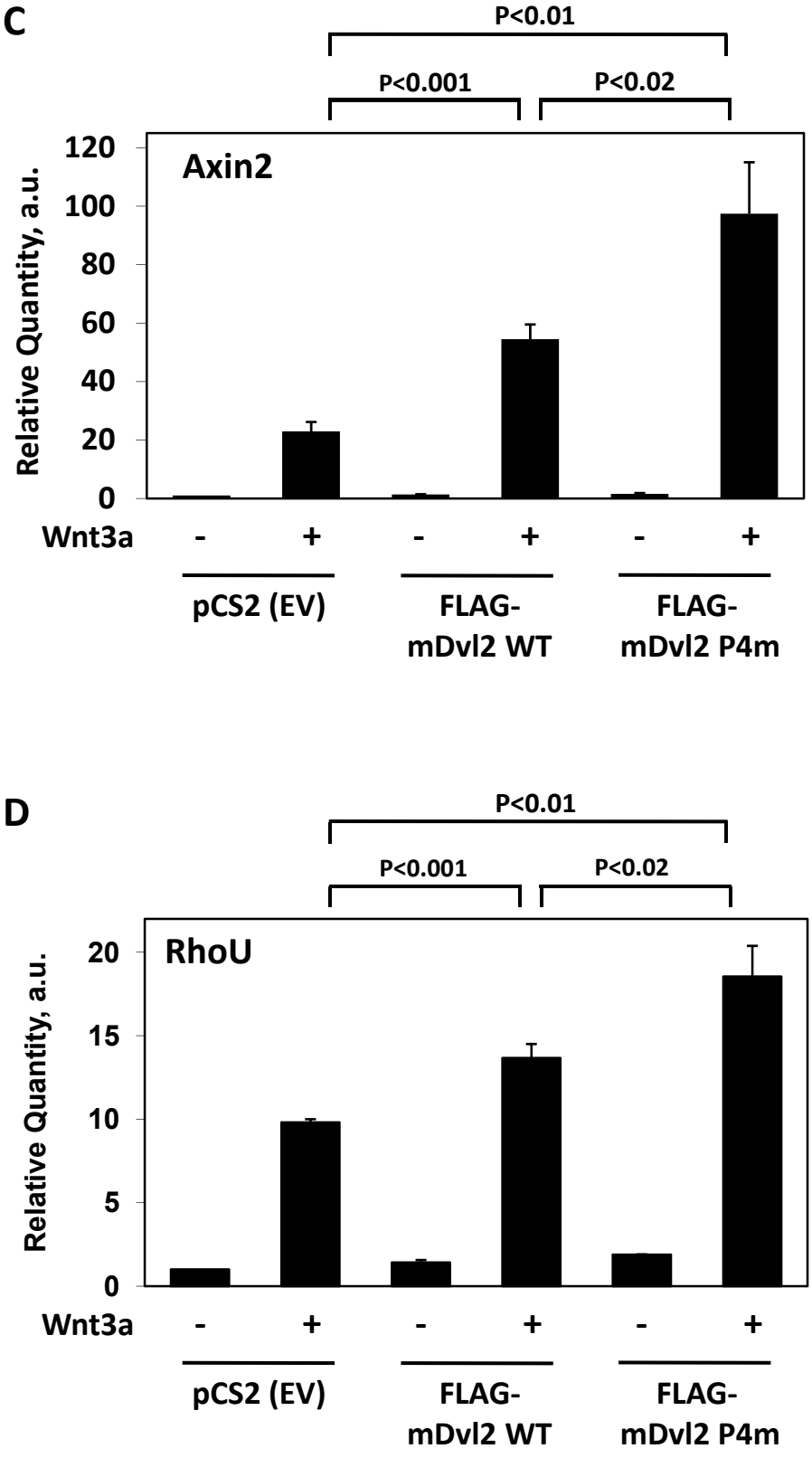
C
P<0.01
P<0.001
P<0.02
Axin2
Relative Quantity, a.u.
120
100
80
60
40
20
0
Wnt3a
-
+
-
+
-
+
pCS2 (EV)
FLAG-
mDvl2 WT
FLAG-
mDvl2 P4m
D
P<0.01
P<0.001
P<0.02
RhoU
Relative Quantity, a.u.
20
15
10
5
0
Wnt3a
-
+
-
+
-
+
pCS2 (EV)
FLAG-
mDvl2 WT
FLAG-
mDvl2 P4m

Figure 5

A

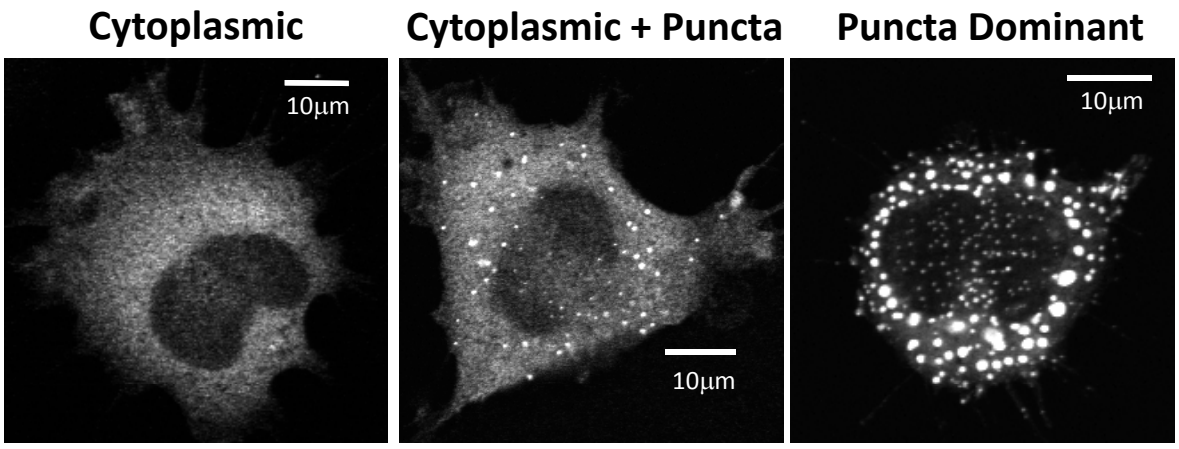
Cytoplasmic
Cytoplasmic + Puncta
Puncta Dominant
10μm
10μm
10μm

B

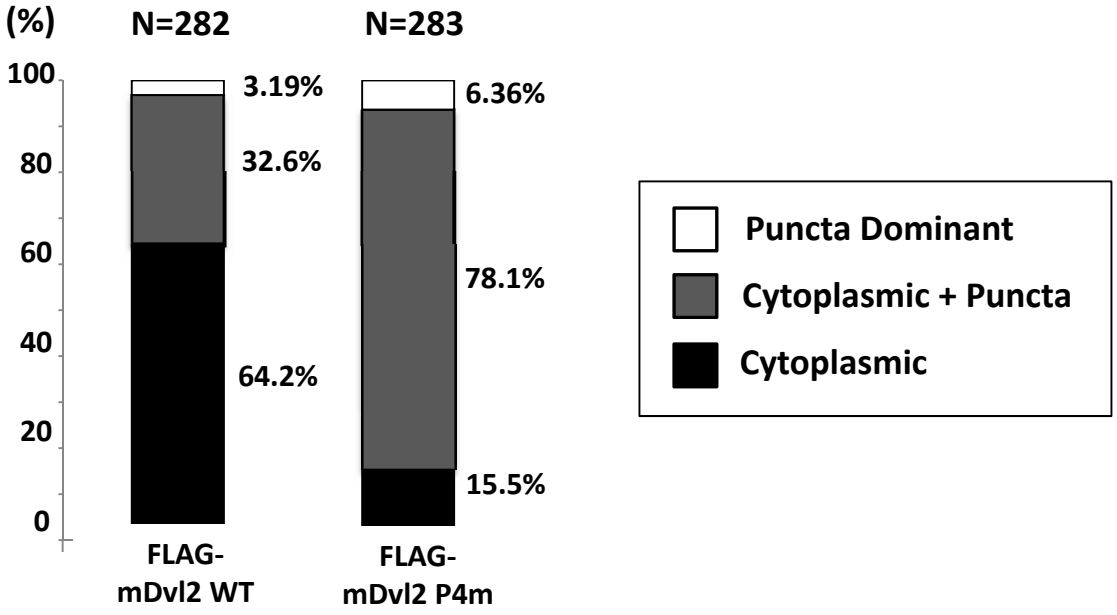
(%)
N=282
N=283
100
80
60
40
20
0
3.19%
32.6%
64.2%
6.36%
78.1%
15.5%
FLAG-
mDvl2 WT
FLAG-
mDvl2 P4m
Puncta Dominant
Cytoplasmic + Puncta
Cytoplasmic

Figure 6

A

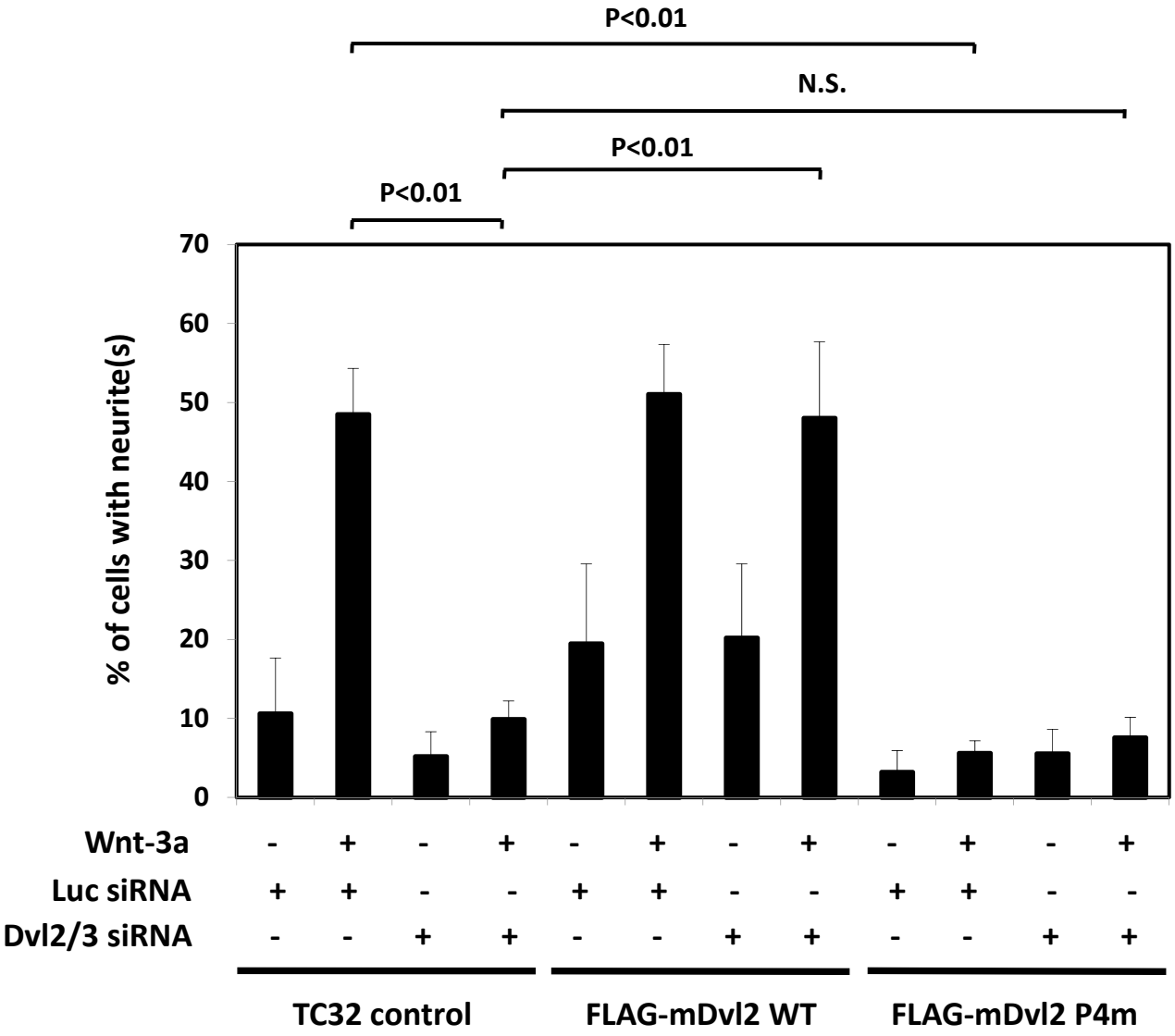
P<0.01
N.S.
P<0.01
P<0.01
% of cells with neurite(s)
70
60
50
40
30
20
10
0
Wnt-3a - + - + - + - + - + - +
Luc siRNA + + - - + + - - + + - -
Dvl2/3 siRNA - - + + - - + + - - + +
TC32 control
FLAG-mDvl2 WT
FLAG-mDvl2 P4m

Figure 6

B

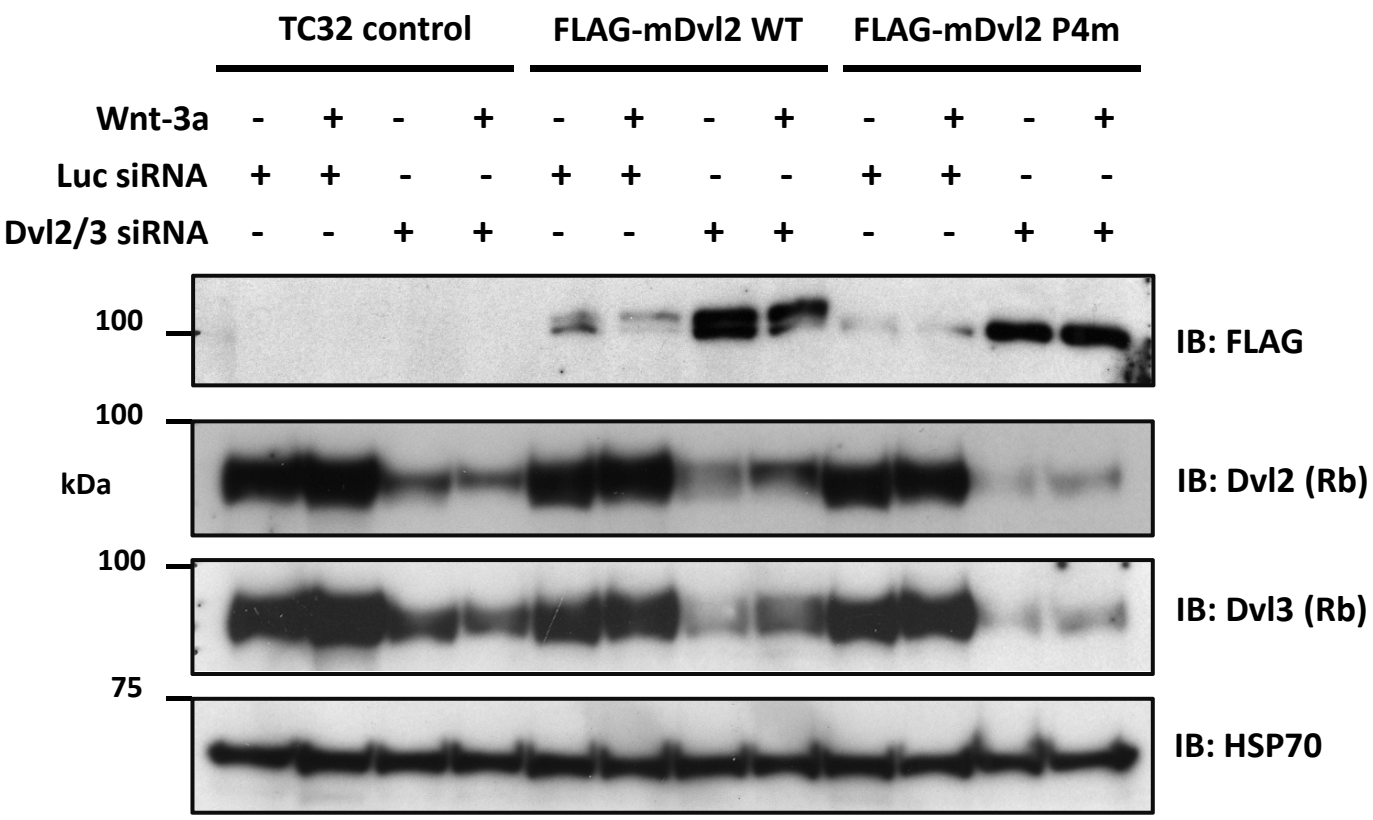
TC32 control
FLAG-mDvl2 WT
FLAG-mDvl2 P4m
Wnt-3a - + - + - + - + - + - +
Luc siRNA + + - - + + - - + + - -
Dvl2/3 siRNA - - + + - - + + - - + +
100
IB: FLAG
100
kDa
IB: Dvl2 (Rb)
100
IB: Dvl3 (Rb)
75
IB: HSP70